Vol. 5 No. 4 Advances in Atmospheric Sciences Nov. 1988

LARGE-SCALE FEATURES OF THE INDIAN SUMMER MONSOON RAINFALL AND THEIR ASSOCIATION WITH SOME OCEANIC AND ATMOSPHERIC VARIABLES

K. D. Prasad and *S. V. Singh*

Indian Institute of Propical Meteorology, Pashan, Pune-411008.

Received April 13, 1987.

ABSTRACT

The summer monsoon rainfall totals for 31 meteorological subdivisions of India for the years 1901–1980 are analysed. The analysis reveals that four leading eigenvectors (EVs) are significant and account for 65% of the total variance.

The spatial pattern of the first EV exhibits in phase fluctuations over almost the whole India. The large coefficients of this vector can be considered as representative of the conditions of large-scale flood and drought over the country. The second pattern reveals the fluctuations mostly over the North Indian region (north of 20° latitude) probably in association with the Western Disturbances. The third pattern indicates fluctuations over the North-West and the North-East India in opposite phase and the fourth pattern exhibits the characteristic features of fluctuations associated with 'break'. The spectral analysis of the coefficients of these EVs revealed quasi-periodicities of 2–5 years.

On the basis of examination of the elements of these EVs the country has been divided into seven homogeneous regions. Rainfall indices of these regions and of the four EVs have been examined for seeking for association with some oceanic and atmospheric variables. The association is significant for the coefficients of the first EV and for the rainfall indices of central and South India. Among all the variables examined, Darwin pressure tendencies have the highest association and appear to be of special significance in prediction of the monsoon rainfall.

I. INTRODUCTION

The Indian summer monsoon is a large scale phenomenon of the Northern Hemispheric summer, during which the country receives most of its annual rainfall. The monsoon rain exhibits large spatial and temporal variation. It sets in over the extreme south of the west coast in the last week of May, progresses northward and is established over the entire country by the first week of July. It remains established during the peak monsoon months of July and August and starts withdrawing from the Indian sub-continent by the middle of September. Even during the established phase of the monsoon, it does not rain every day. The quasi-stationary monsoon trough keeps on changing its latitudinal position resulting in varying rainfall patterns over the country. Small synoptic scale systems such as lows and depressions modify this general rainfall pattern. During the northernmost swing of the monsoon trough copious rainfalls over the northern sub-mountainous regions and the southeast tip of the peninsula and it is deficient over the central parts of the country. This situation is typically known as a monsoon 'break'. Occasionally, the mid-latitude disturbances, known as 'Western Disturbances' also traverse the country causing rainfall over the northern parts of it.

Generally, the three aspects of the seasonal monsoon rainfall, viz. the spatial distribution, the temporal fluctuation and the prediction, are of particular interest. Subbramayya (1968) found that rainfall of the north-east India has opposite relation with that of the west and central India. This was further elaborated by Bedi and Bindra (1980) who determined the eigenvectors and their temporal coefficients using station data. Since monsoon is a planetary scale phenomenon, it has been related to several global scale variables. The variables related to the Southern Oscillation and the Northern Hemispheric surface air temperature have received particular attention. Shukla and Paolino (1983) found Darwin pressure tendency from winter to spring as a good indicator of the monsoon rainfall. Mooley and Parthasarathy (1983) found that the indices of dryness and wetness over India show significant correlation with the Southern Oscillation index and with the sea-surface temperature anomaly of the equatorial eastern Pacific for the concurrent and the succeeding seasons (autumn). Rasmusson and Carpenter (1983) considered the monsoon precipitation data of 31 Indian subdivisions and of 35 Indian and Sri Lanka stations to study the relationship between the equatorial Pacific warm episodes (El-Nino) and the precipitation over India and Sri Lanka.

In the present study the technique of empirical orthogonal function (EOF) has been applied to the summer monsoon rainfall of meteorological subdivisions of contiguous India to identify quantitatively the statistically significant spatio-temporal features of the monsoon rainfall. The EOFs are examined for identifying homogeneous regions of precipitation and their time coefficients are analysed for potential periodic behaviour. Finally, they are correlated with some oceanic and atmospheric large-scale variables in a search for possible predictive relationships.

II. DATA

The monthly rainfalls of 31 contiguous meteorological subdivisions (Fig. 1) of India for the summer monsoon season (June through September) for years 1901–1980 are obtained from the India Meteorological Department. After proper scrutiny for gross errors etc. these data are put on the magnetic tape. Area weighted monthly rainfalls are prepared for each of the subdivisions by multiplying the rainfall by the ratio of the area of the corresponding subdivision to the area of total India. Symbolically it can be represented as

$$R^*_{ij} = R_{ij} \times A_i \Big/ \sum_{k=1}^{31} A_k,$$

where R^*_{ij} is the revised and R_{ij} is the original rainfall for ith subdivision and jth year. A_i is the area of ith subdivision and denominator shows the total area of India. The summer monsoon seasonal rainfall series for each subdivision is, then, obtained by simple averaging of these revised monthly data.

The monthly surface temperature anomalies (1901–1980) averaged over the whole Northern Hemisphere (NHSAT) used in this study are taken from Jones (1985a). The data of the seasonal (August-October) Atlantic hurricane frequencies, the tropical storm frequencies and the El-Nino events (moderate and strong) off the South American coast for the period 1901–1980, used in the study, are taken from Gray (1983).The data for Darwin pressure have been obtained from Climate Analysis Centre, USA. Arctic region surface air temperature and Southern Hemisphere sea-surface temperature have been obtained from

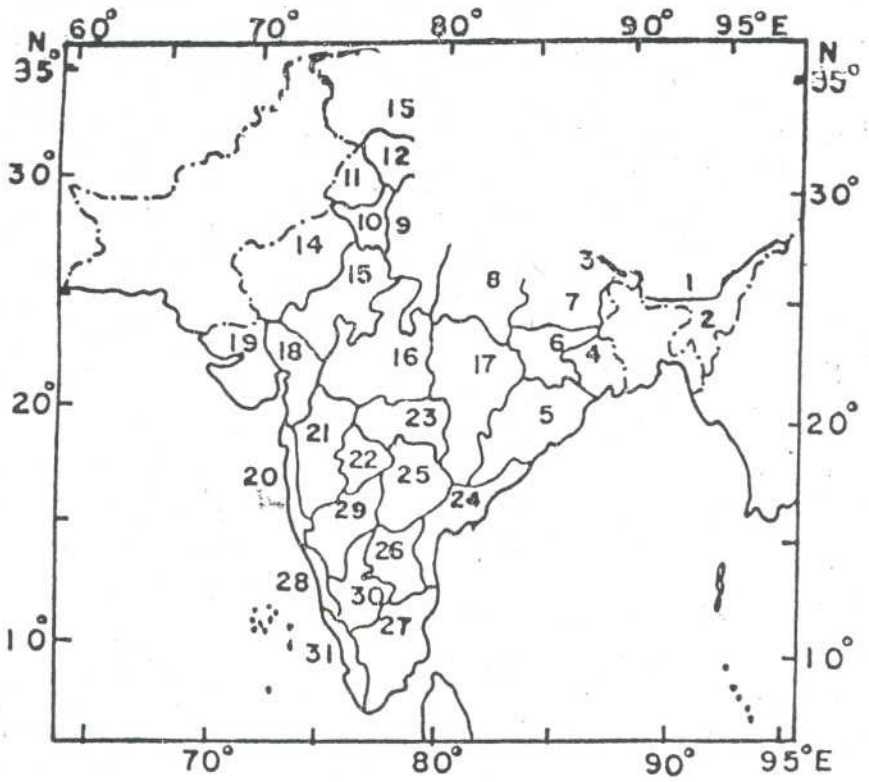

1 NORTH ASSAM	11 PUNJAB	21 MADHYA MAHARASHTRA
2 SOUTH ASSAM	12 HIMACHAL PRADESH	22 MARATHWADA
3 SUB-HIM. W. BENGAL	13 JAMMU & KASHMIR	23 VIDARBHA
4 GANGETIC W. BENGAL	14 RAJASTHAN WEST	24 COASTAL A. P.
5 ORISSA	15 RAJASTHAN EAST	25 TELENGANA
6 BIHAR PLATEAU	16 MADHYA PRADESH (W)	26 RAYALASEEMA
7 BIHAR PLAIN	17 MADHYA PRADESH (E)	27 TAMIL NADU
8 U. P. EAST	18 GUJARAT	28 COASTAL MYSORE
9 U. P. WEST	19 SAURASHTRA & KUTCH	29 INTERIOR MYSORE (N)
10 HARYANA	20 KONKAN	30 INTERIOR MYSORE (S)
		31 KERALA

Fig. 1. Rainfall of 31 meteorological subdivisions of India considered in the analysis.

III. LARGE-SCALE FEATURES OF THE SUMMER MONSOON RAINFALL

The EOF analysis of the rainfall co-variances between the 31 meteorological sub-divisions provided the number of eigenvectors (EVs) equal to the number of space points (31 in this case). The technique followed is the same as that of Sikka and Prasad (1981). All these EVs may not contain significant information because most information is contained in the leading EVs with the largest eigenvalues. The importance of higher order EVs diminishes and the association between the EV and the physical processes becomes more difficult to explain as the pattern contains more noise of the field. Thus, it is important to know how many of these are statistically different from the noise. This has been achieved by performing the Monte Carlo Simulation using 100 trials as done by Barnett and Preisendorfer (1978). The Monte Carlo curves for 95% and 5% significant levels are plotted

in Fig. 2 along with the actual eigenvalue curve obtained from the original data. The plot shows the first four EVs as significant. Also, the first three EVs are found distinct from each other when tested by the criteria of North et al. (1982). However, the third and the fourth EVs do not satisfy this criteria of separability. The fourth EV pattern, however, appears to be important as it reveals one of the important features of the summer-monsoon rainfall variation, the 'break'. Hence, the first four EVs are retained for further analysis in the present study.

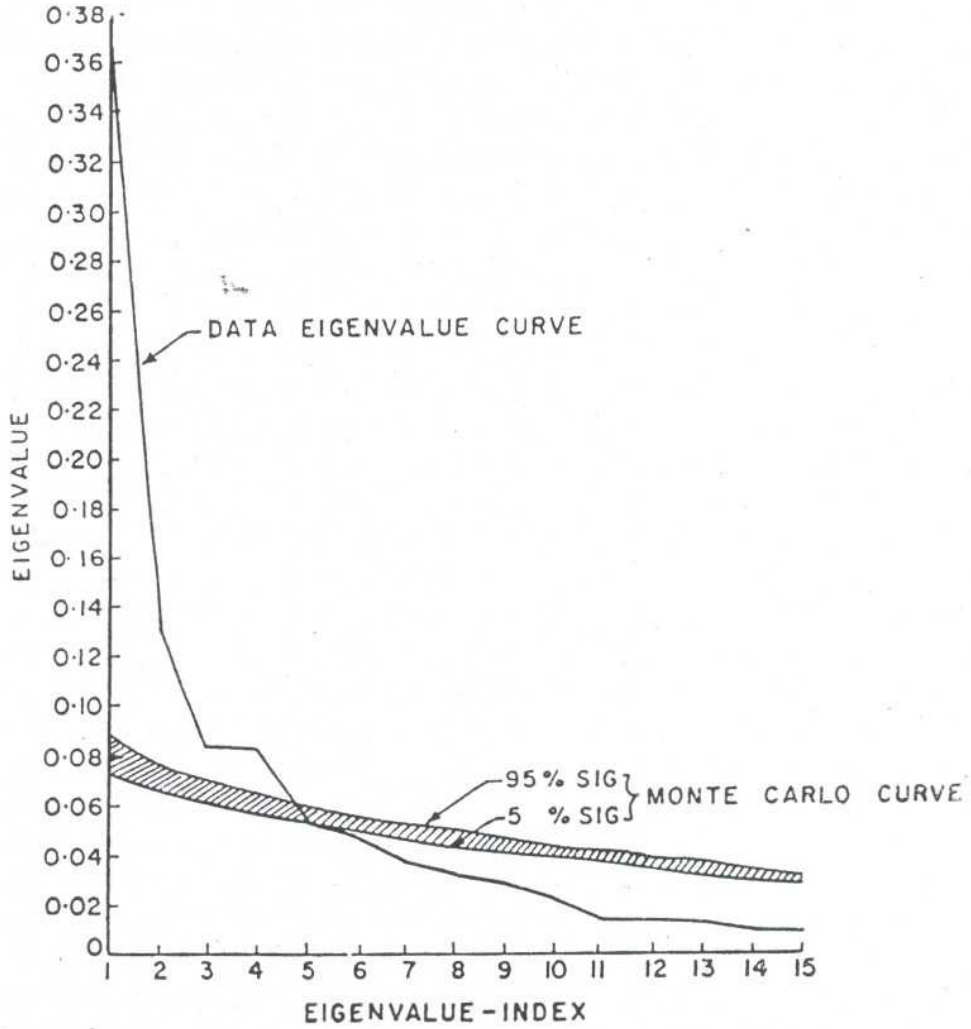

Fig. 2. Eigenvalue versus eigenvalue-index for rainfall data and Monte Carlo simulation.

These four EVs together account for 65% of the total variance (Fig. 3) which is higher in comparison with the corresponding 47% described by the first four EVs of Bedi and Bindra (1980). This is because they used station rainfall data which exhibit a higher degree of spatial variability as compared to the spatially averaged data used in the present study.

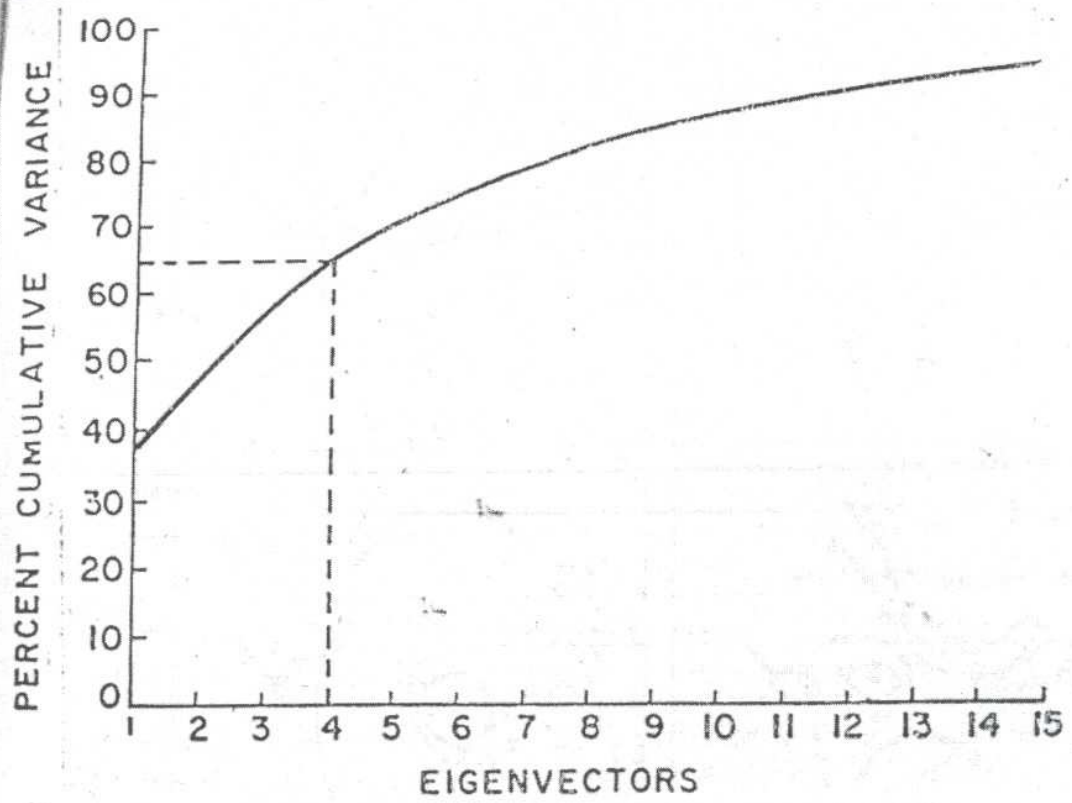

Fig. 3. Cumulative variance in percent plotted for the first fifteen eigenvectors.

1. *The First Eigenvector (EV1)*

EV1 (Fig. 4) which explains 37% of the total variance shows an opposite relationship between rainfall over the north-east India and that over the rest of India. This type of distribution of the seasonal rainfall anomaly over India is also evidenced from the results of Bedi and Bindra (1980) and Rasmusson and Carpenter (1983). Since covariance matrix has been used the pattern of EV1 is also similar to the distribution of standard deviation (Fig. 5). As the southernmost position of the monsoon trough results in abundance of rainfall over the central and the adjoining areas and reduced rainfall over the north-east, it appears that the EV1 characterizes the rainfall distribution associated with the monsoon trough.

The time coefficients of the first four EVs are plotted in Fig. 6. The smooth curves in the figure show nine term Gaussian filtered series and the horizontal dashed lines show ± 1.0 Standard Deviation (SD). As EV1 explains a substantial amount of the total variance and a negative (positive) coefficient associated with EV1 indicates abundance (little) of rainfall over almost the whole of India, the coefficients can be used as an indicator of large-scale behaviour of the monsoon over the country. Thus, it can be seen from the figure that the coefficients are negative ≤ -1.0 SD in the years 1916, 1917, 1919, 1933, 1942, 1955, 1961 and 1975. The monsoon was quite pronounced during these years. Similarly, in the years 1902, 1905, 1907, 1911, 1913, 1918, 1920, 1941, 1951, 1965, 1972, 1974 and 1979

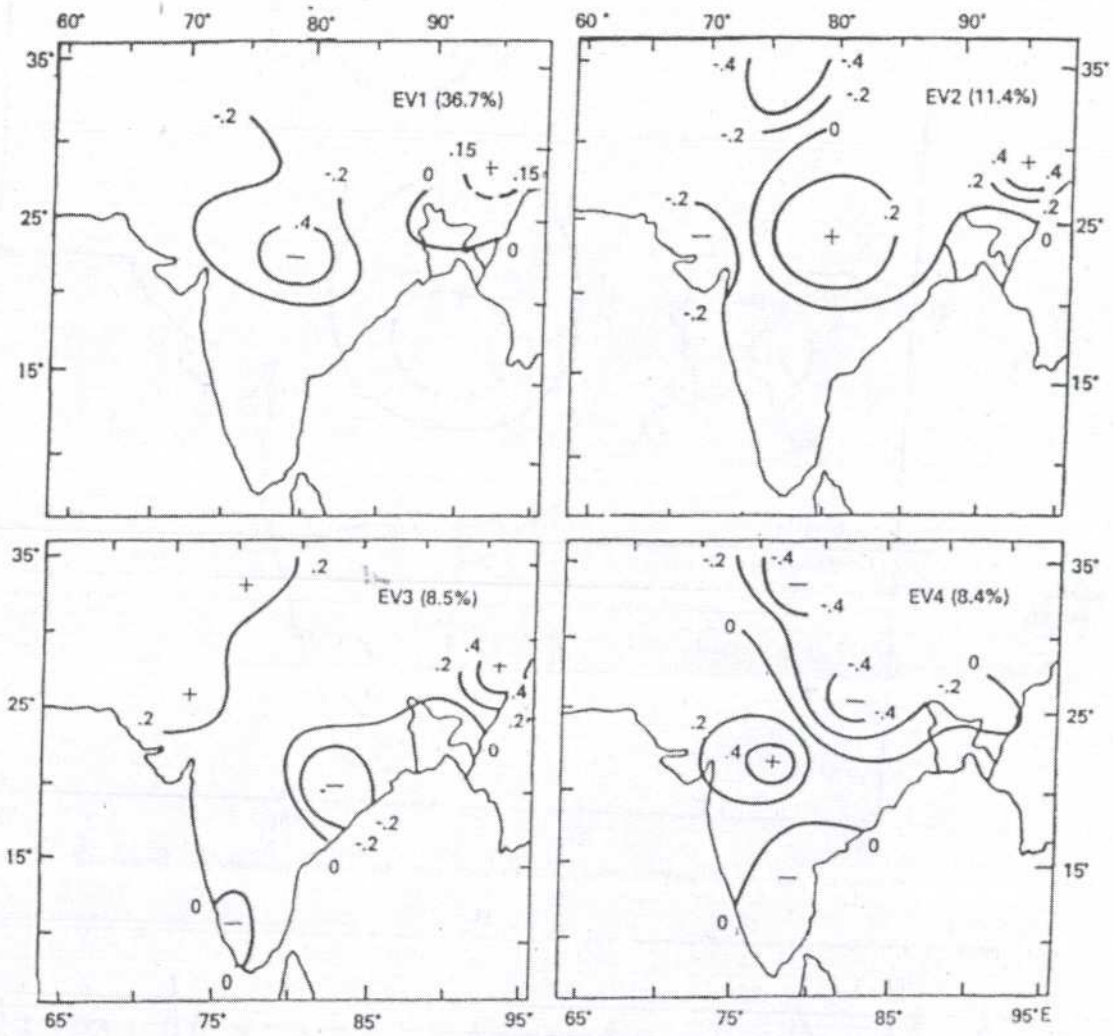

Fig. 4. The first four statistically significant eigenvector (EV1–EV4) patterns of the summer-monsoon rainfall anomalies. The variance explained by each of the EVs is shown in parenthesis.

the coefficients are positive$\geqslant$1.0 SD, and the monsoon activities were quite poor during these years. The coefficients also show a decreasing linear trend till the year about 1950 followed by an increasing trend thereafter. The trend is more conspicuous in ten year running means of the coefficients, not presented here. The area weighted rainfall of India also shows a similar feature.

2. *The Second Eigenvector (EV2)*

The EV2 (Fig. 4) explains 11% of the total variance and shows rainfall variation over central Indian and adjoining foothills of Himalayas in opposite phase to that over Gujarat, Saurashtra and Kutch and Jammu and Kashmir. Large loadings are confined to the north of 20°N latitude. The pattern probably depicts the characteristic features of the Western Disturbances which continue to cause significant rainfall over the north India even during the monsoon season. The pattern also suggests that the disturbances over Jammu and Kashmir favour the development of disturbances over Gujarat and Saurashtra and Kutch.

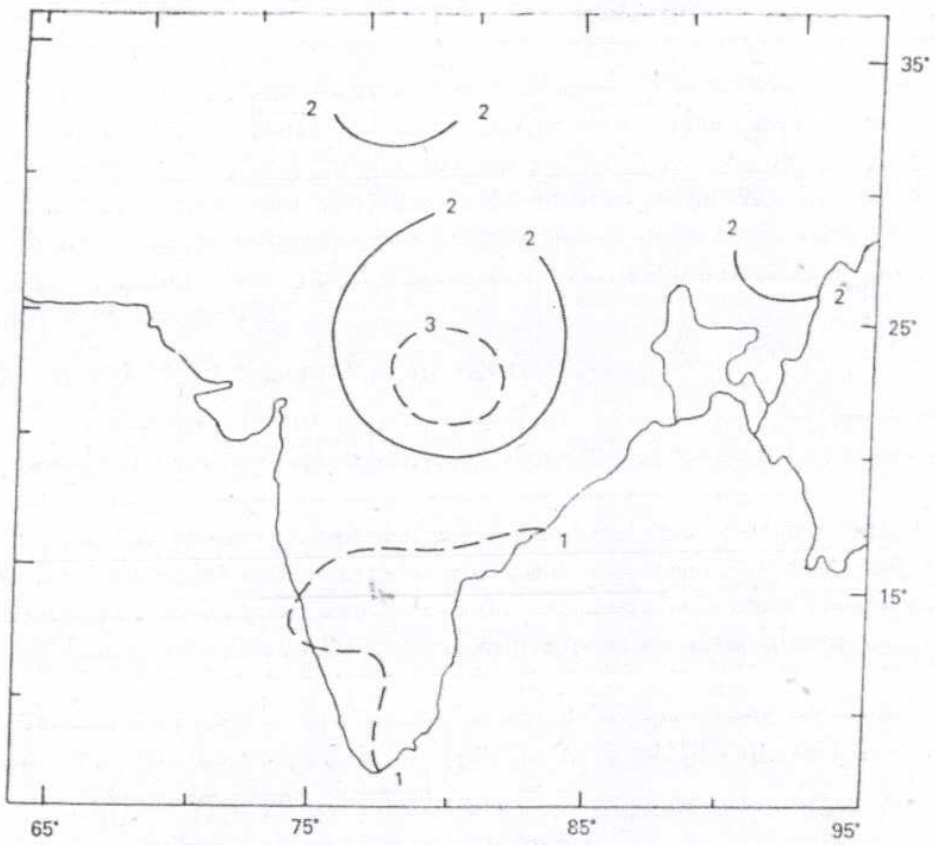

Fig. 5. Standard deviation map of rainfall (1901–1980). The units are in cm.

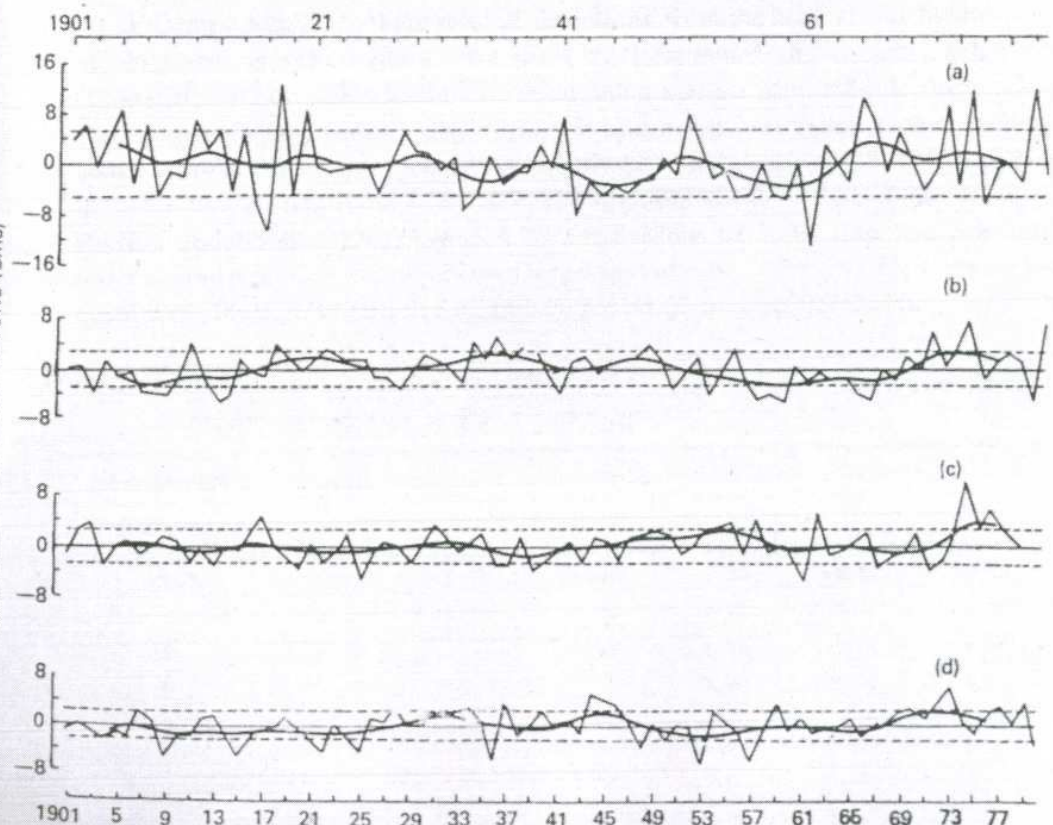

Fig. 6. Time-varying coefficients corresponding to (a) the first (b) the second (c) the third and (d) the fourth EVs. The smooth curves show nine point Gaussian filtered series and the horizontal dashed lines denote ±1 S.D.

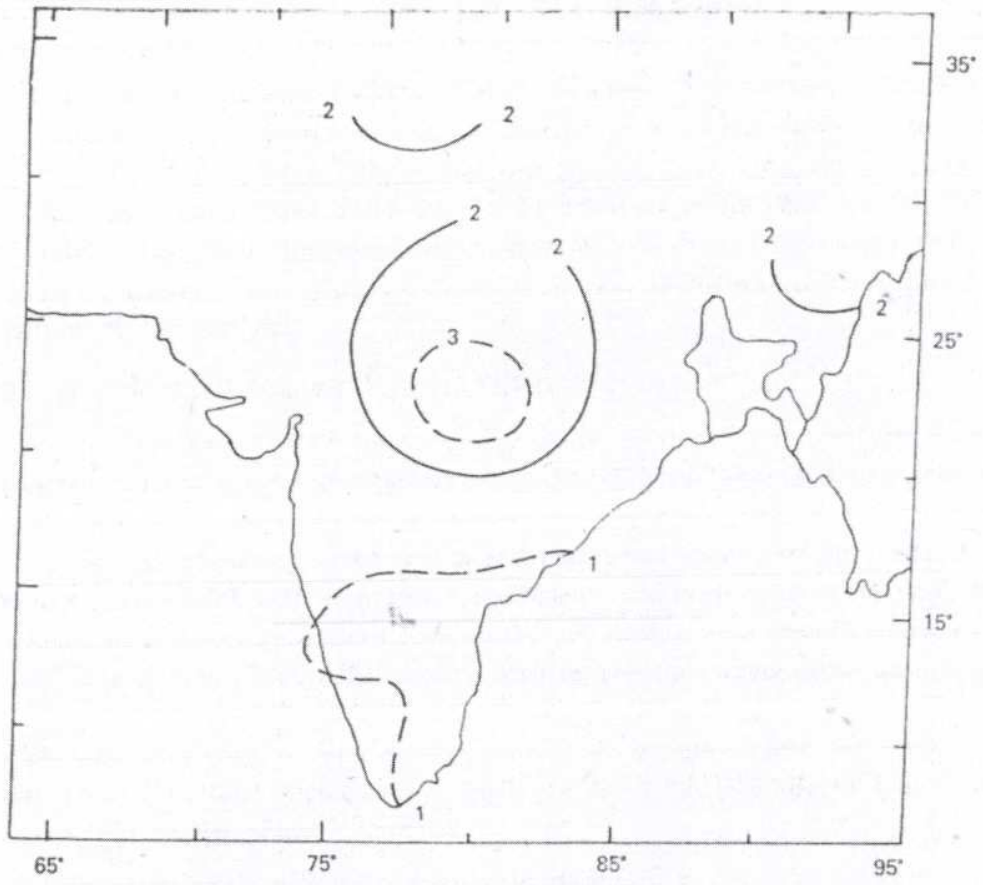

Fig. 5. Standard deviation map of rainfall (1901–1980). The units are in cm.

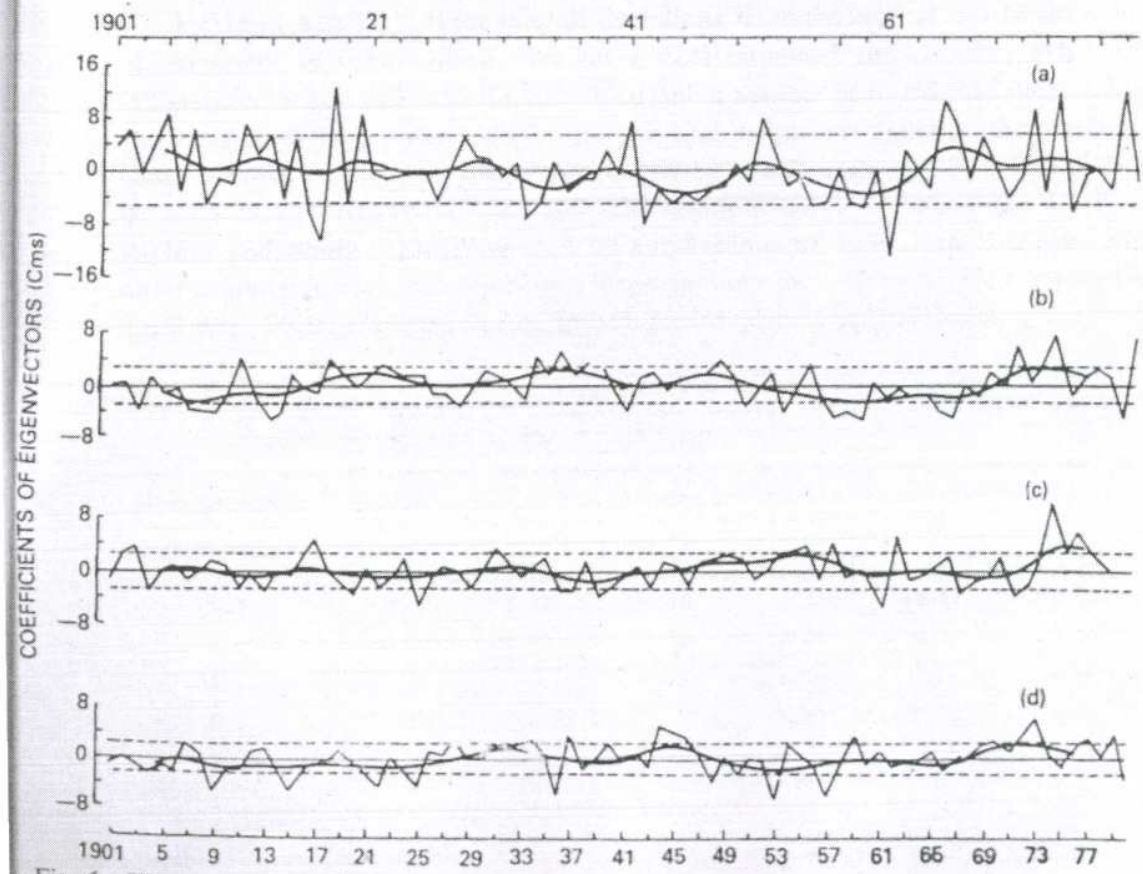

Fig. 6. Time-varying coefficients corresponding to (a) the first (b) the second (c) the third and (d) the fourth EVs. The smooth curves show nine point Gaussian filtered series and the horizontal dashed lines denote ±1 S.D.

The associated time coefficients (Fig. 6) show large positive (≥ 1.0 SD) values during the years: 1911, 1918, 1934, 1936, 1938, 1939, 1948, 1955, 1971, 1973, 1974 and 1980. As seen from the pattern, rainfall is more over northern India than over the rest of India during these years, most likely due to the activities of the Western Disturbances over the country. The result suggests that the activities of these disturbances were more frequent generally during the periods 1916 to 1950 and 1968 onward than during the remaining period of the analysis.

3. *The Third (EV3) and the Fourth (EV4) Eigenvectors*

The pattern of EV3 shows similarity in variation over northern Assam and north-western India whereas the variation over east Madhya Pradesh, Orissa and adjoining areas happens to be in opposite phase to that over the other parts of the country.

The EV4 appears to represent a well-recognised feature of the monsoon rainfall. The pattern, associated with a negative coefficient, shows more rainfall along the foothills of Himalayas and over the eastern parts of the peninsular India which generally happens during the 'break'. When the coefficients are positive, generally favourable location of the monsoon trough and traverse of the monsoon depressions is indicated. The coefficients associated with these EVs (Fig. 6) have smaller amplitudes compared with the coefficients of the first two EVs. The time coefficients of both the third and the fourth EVs show slight rising trends during the period examined.

IV. HOMOGENEOUS PRECIPITATION REGIONS

It is quite possible that the rainfall deviations from the normal may be similar in a number of neighbouring sub-divisions. Walker (1924) examined the correlation between the rainfall in different parts of Indo-Burma region and a number of worldwide meteorological factors and considered Peninsular India, north-east and north-west India as three different homogeneous areas for developing regression equations. Subbramayya (1968) found that rainfall of the west and central India behaves in the opposite sense to that of the north-east India. Paolino and Shukla (1981) grouped 29 subdivisions of India into five coherent regions in order to study rainfall variability on a larger spatial scale. These regions are northeast India, north-west India, southern India, Indian peninsula and central India.

Table 1. Correlations between the Area-weighted Summer-monsoon Rainfalls of Seven Homogeneous Regions (as indicated in Fig. 7) of India

Homogeneous Regions	1	2	3	4	5	6	7
1	1.00	−0.42	−0.07	−0.23	−0.23	−0.29	−0.03
2		1.00	0.26	0.22	0.37	0.20	−0.09
3			1.00	0.42	0.47	0.18	0.24
4				1.00	0.56	0.58	0.56
5					1.00	0.63	0.39
6						1.00	0.65
7							1.00

In the present study, we identify the spatial coherent regions of precipitation over India by examining the elements of significant EVs for the study of their rainfall behaviour. The region over which the sign of the element of the EVs remained unchanged in case of each of the four significant EVs may be regarded as homogeneous. The analysis shows seven regions over which the seasonal precipitation variations are more or less coherent. These regions are shown in Fig. 7. The correlation coefficients between area weighted rainfalls of the regions are presented in Table 1. The table shows that the intercorrelations among these regions are generally low. The highest correlation of 0.65 is obtained between the regions six and seven. However, synoptic experience says that these two regions are generally in different weather regimes in the sense that when monsoon is active over one it is weak over the other and vice-versa. Hence, they are classified into two separate homogeneous regions.

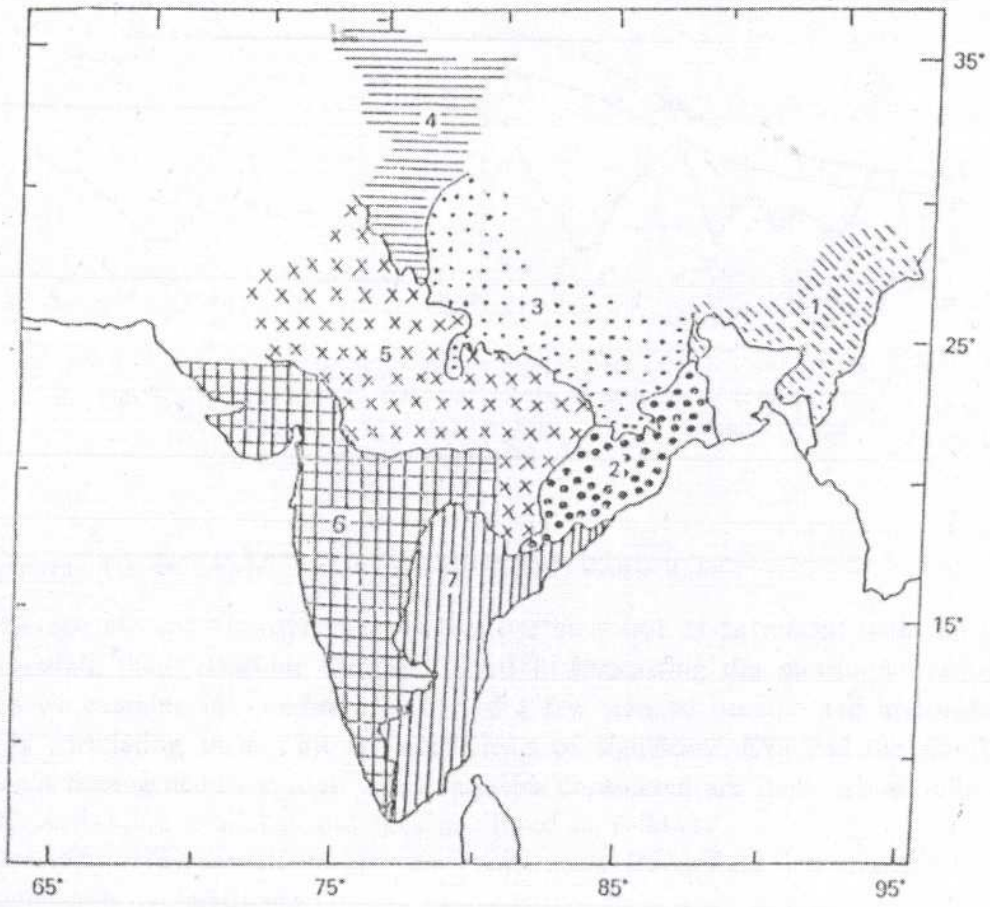

Fig. 7. The seven homogeneous regions of precipitation over India.

V. SPECTRAL ANALYSIS

In order to identify the major time scales in the fluctuation of the seasonal precipitation over India, the time-dependent coefficients of the four EVs are subjected to spectral analysis. Fig. 8 depicts the plot of spectral estimates versus time lag and period. The coefficients corresponding to the EV1 show spectral peak at 2.8 year and 2.3 year, significant at 5%

and 10% level respectively. The spectrum for the coefficients corresponding to the EV2 has a major peak at 3.2 year which is significant at 5% level. The coefficients corresponding to the EV3 and EV4 show peaks at 3.7 year and 4.8 year respectively, both significant at 10% level. It is noted that all the four time coefficients exhibit peaks corresponding to the quasi-biennial oscillation.

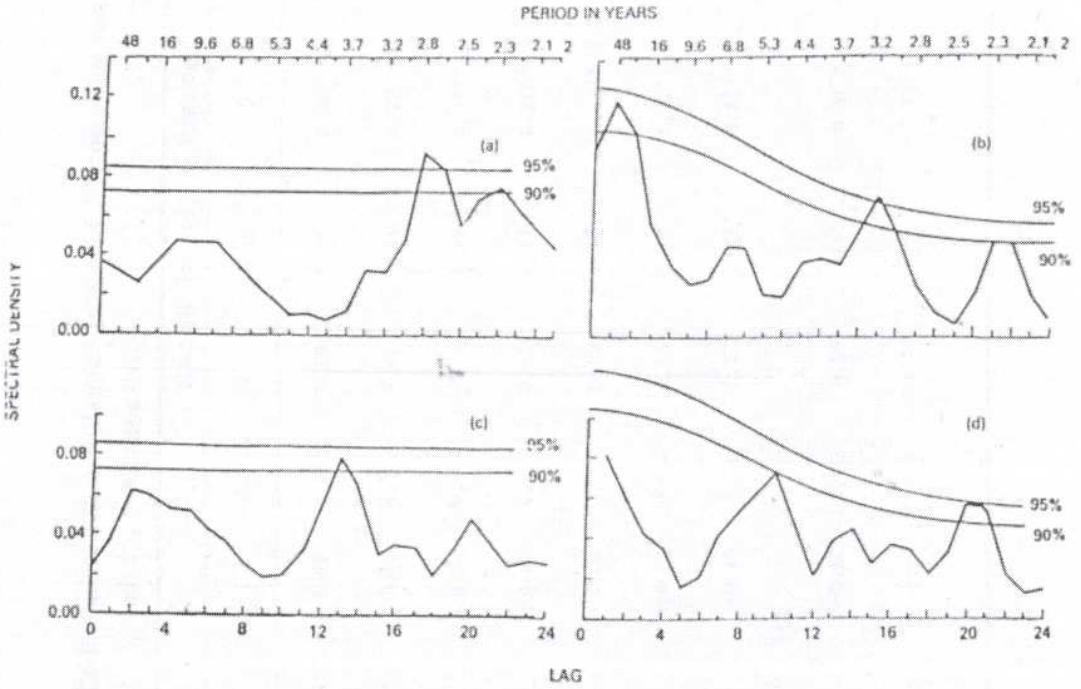

Fig. 8. Spectral density estimates of the time series of coefficients corresponding to (a) the first, (b) the second (c) the third and (d) the fourth EVs.

VI. RELATIONS TO OCEANIC AND ATMOSPHERIC VARIABLES

If some oceanic and atmospheric variables are identified to be related with the Indian monsoon rainfall, these relations can be utilised in forecasting the monsoon rainfall. In this section we examine the predictive utility of a few selected oceanic and atmospheric variables by correlating them with the coefficients of significant EVs and the rainfall indices of seven homogeneous regions. The variables considered are those whose long series (1901–1980) record are available and they are listed as follows:

(i) Northern Hemispheric surface air temperature (Jan., Feb. and average for Jan. and Feb.) – (NHSAT)
(ii) Storm and hurricane frequencies in West Atlantic.
(iii) El Nino events off the west coast of South America.
(iv) Darwin sea-surface pressure tendencies (May–Jan.).
(v) Arctic region (65°N to 85°N) surface air temperature (Jan.)–(ASAT).
(vi) Southern Hemisphere (2.5°S to 62.5°S) sea-surface temperature (Jan.) – (SHSAT).

The correlations are presented in Table 2. It can be seen from the table that all the variables have significant association with the coefficients of EV1. The correlations between the coefficients of EV1 and NHSAT (January and average of January, February) are signif-

Table 2. Correlations of Oceanic and Atmospheric Variables with the Coefficients of EVs and Rainfall Indices of Homogeneous Regions of India. The double star (**) and single star (*) represent significance at 1% and 5% level respectively

	Variables	Coefficients of				Rainfall Indices of Regions						
		EV1	EV2	EV3	EV4	1	2	3	4	5	6	7
NHSAT	Jan.	−0.35**	0.04	0.11	0.12	−0.06	0.03	0.19	0.17	0.36**	0.40**	0.28*
	Feb.	−0.25*	−0.02	0.13	0.07	0.05	0.13	0.03	0.14	0.22	0.29*	0.22
	Jan. & Feb.	−0.35**	0.00	0.14	0.11	0.00	0.09	0.13	0.18	0.34**	0.40**	0.29*
	ASAT (Jan.)	−0.31*	0.21	0.03	0.19	−0.05	0.05	0.20	0.04	0.35**	0.23	0.02
	SHSAT (Jan.)	−0.32**	0.02	0.08	0.36**	0.10	0.13	0.00	0.10	0.35**	0.36**	0.12
	Hurricane Frequencies	−0.31*	−0.02	0.14	0.06	−0.11	0.00	0.15	0.19	0.27*	0.30*	0.30*
	Storm & Hurricane Frequencies	−0.38**	0.00	0.12	0.05	−0.12	0.03	0.22	0.25*	0.32**	0.39**	0.32**
	El Nino Events	−0.39**	0.05	0.11	0.22	−0.07	0.06	0.19	0.13	0.40**	0.47**	0.26*
	Darwin Pressure Tendencies (May-Jan.)	0.40**	0.06	−0.07	0.07	0.13	−0.13	−0.25*	−0.35**	−0.33**	−0.31*	−0.43**

ficant at 1% level. The negative correlations indicate that warmer NHSAT in winter is followed with excess monsoon rainfall and vice-versa. ASTA (January) and SHSAT (January) also show significant correlations with the coefficients of EV1 though, their magnitudes are less than that for NHSAT. SHSAT also shows significant association with the coefficients of EV4. Hence, it can be utilised in forecasting the coefficients of EV1 as well as EV4.

Significant negative correlations in both the cases of Atlantic storms suggest that Indian monsoon is active in those years in which the storms are more frequent. However, the Indian monsoon is more closely related to the total number of storm and hurricane frequencies than that of hurricane alone.

The El Nino-Southern Oscillation (ENSO) is a major climatic event which affects the atmospheric circulation all over the world. The inter-annual variability of the Indian summer monsoon has been linked with this planetary scale feature. Mooley and Parthasarathy (1983) found that severe drought condition prevails over India during the years of strong El Nino events. In order to have a quantitative measure of the association, we quantified severe, moderate and non-El Nino events by assigning to them indices -4, -2 and zero respectively following Gray (1983) and correlated the resulting time series with the coefficients of EVs. The correlation with the coefficients of EV1 (Table 2) is significant at 1% level. This shows that the Indian monsoon, which is observed before the commencement of El Nino event (generally during December), is generally weak in the year of El Nino. It appears that monsoon rainfall can not be forecast from such a relationship. However the warming in the sea-surface temperature off the Peru Coast which culminates into El Nino event generally shows its first signs in April-May. Hence, the early detection of the conditions favourable for the occurence of El Nino event will be useful in prediction of the monsoon rainfall.

Since El Nino is an event occurring at irregular intervals it does not help much in continuous monitoring of the changes that take place in the atmospheric-oceanic system. It is known that El Nino represents a peak phase of a more general short term climatic fluctuation known as the Southern Oscillation. Hence, we have also correlated the coefficients of EV3 with the pressure index of the Southern Oscillation. The pressure of Darwin or the difference of pressure between Tahiti and Darwin can be considered as the indices of Southern Oscillation. A long record of Tahiti pressure is not available and the correlation between spring Tahiti pressure and the Indian monsoon rainfall for the available record was negligibly small. Hence, we correlated Darwin pressure as its long term record is considered more reliable (Trenberth, 1976). The monthly Darwin pressure showed a maximum negative correlation ($cc = -0.26$.) with the coefficients of EV1 in January and the correlation changes sign for the subsequent months leading to a high positive value ($cc = 0.32$) for May. Hence, we examined the May minus January Darwin pressure tendency for relationship with rainfall. The correlation (Table 2) between the pressure tendencies and the coefficients of EV1 is rather higher than those for Darwin pressure for May or January alone. Also, it is seen that Darwin pressure tendencies have the highest association with the coefficients of EV1 among all the variables examined.

Further, in order to examine the areas of major influence, the variables are correlated with the rainfall index of each of the homogeneous regions (Fig. 7) of India. The results (Table 2) show that the rainfall of regions 1 to 4 have poor association with these variables except for Darwin pressure tendencies showing association with regions 3 and 4 and

Table 3. Correlations of Oceanic and Atmospheric Variables with the Coefficients of EVs and Rainfall Indices for the Two Periods of the Data Sample: The upper value corresponds to the period 1901–1940 and the lower one to the period 1941–1980. Double star and single star represent significant at 1% and 5% level respectively

	Variables	Coefficients of				Rainfall Indices of Regions						
		EV1	EV2	EV3	EV4	1	2	3	4	5	6	7
NHSAT	Jan.	−0.21	0.05	0.08	0.19	−0.11	0.02	0.06	0.03	0.23	0.34*	0.21
		−0.50**	0.05	0.11	0.02	0.02	0.06	0.35*	0.34*	0.47**	0.44**	0.32*
	Feb.	−0.06	0.01	0.19	0.26	0.20	−0.04	−0.21	−0.11	0.08	0.25	0.22
		−0.43**	−0.06	0.00	−0.15	−0.04	0.31*	0.32*	0.44**	0.36*	0.32*	0.21
	Jan. & Feb.	−0.20	0.04	0.16	0.17	0.05	−0.01	−0.08	−0.05	0.18	0.35*	0.25
		−0.53**	0.00	0.06	−0.07	−0.01	0.21	0.38*	0.44**	0.47**	0.43**	0.30
	ASAT (Jan.)	0.12	0.27	−0.14	0.20	−0.13	0.07	0.09	−0.16	0.16	0.07	−0.19
		−0.49**	0.18	0.15	0.17	0.02	0.05	0.33**	0.25	0.53**	0.39*	0.27
	SHSAT (Jan.)	−0.43**	−0.13	0.14	0.36*	−0.13	0.07	−0.05	0.26	0.43**	0.58**	0.24
		−0.23	0.16	−0.11	0.27	−0.00	0.23	0.06	0.02	0.28	0.13	−0.09
	Hurricane Frequencies	−0.36*	−0.05	0.25	0.05	0.01	0.08	0.16	0.29	0.34*	0.31*	0.35*
		−0.26	0.02	−0.10	−0.08	−0.16	−0.07	0.21	0.16	0.19	0.25	0.18
	Storm & Hurricene	−0.39*	0.02	0.18	0.09	−0.07	0.07	0.18	0.27	0.36*	0.37*	0.26
	Frequencies	−0.41**	−0.01	−0.09	−0.16	−0.13	0.02	0.37*	0.33*	0.28	0.43**	0.38*
	El-Nino Events	−0.43**	−0.26	0.32*	0.23	−0.25	−0.01	0.13	0.27	0.38*	0.60**	0.33*
		−0.37*	0.33*	−0.06	0.21	0.08	0.13	0.26	0.01	0.42**	0.34*	0.19
	Darwin Pressure	0.27	0.16	−0.24	0.30	0.15	0.09	−0.19	−0.40**	−0.17	−0.18	−0.47*
	Tendencies (May–Jan.)	0.50**	−0.02	0.11	−0.04	0.12	−0.32*	−0.33*	−0.34*	−0.45**	−0.39*	−0.38*

Atlantic total storm frequencies with the region 4. Darwin pressure tendencies show a wide range of spatial influence which varies from region 3 to 7. Also, most of the variables indicate significant correlation at 1% level with the rainfall index of regions 5 to 7. The variables examined, thus, can be useful in predicting the rainfall index of these regions.

The correlation coefficients may change either due to the long term climatic trend or due to random fluctuations in the data samples. Hence, to examine the stability of the above relationships we have recomputed the correlation coefficients by splitting the data samples into two (1901–1940 and 1941–1980) halves (Table 3). The table shows that the association of the Indian monsoon rainfall with SHSAT (January) and Hurricane frequencies is better over the period 1901–1940 whereas over the period 1941–1980 Darwin pressure tendencies, NHSAT (winter) and ASAT (January) show better association with the Indian monsoon rainfall. The association is rather good for both the periods in case of El Nino events and storm and hurricane frequencies. The results thus, suggest that the recent 40 years of data of these variables are more useful in predicting the Indian monsoon rainfall.

VII. CONCLUSION

The study reveals that the complex temporal and spatial fluctuations of the Indian summer monsoon rainfall can be described with the help of four significant leading EVs, which account for 65% of the total variance. The patterns corresponding to these EVs are consistent with the observed synoptic patterns. The coefficients of the most leading EV provide the index of flood and drought over the country which can be advantageous over that obtained by averaging rainfall on all India basis and can be used in further investigation and prediction work. Also the monsoon fluctuations show a quasi-periodic behaviour of 2–5 years superposed on a long term trend.

We have identified the homogeneous regions of precipitation over India. The scheme appears to be satisfactory. Precipitation variations within each of the regions are relatively uniform and hence the rainfall indices of these regions can be forecasted with a better accuracy than that of individual subdivision by a suitable statistical scheme.

We have also found that coefficients of EV1 are associated with NHSAT (Jan., Feb. and average of Jan. Feb.), SHSAT (Jan.), ASAT (Jan.), Atlantic storm frequencies and Southern Oscillation indices (El Nino and Darwin pressure tendencies). The strongest association is that with Darwin pressure tendency and it is the best predictor of the Indian monsoon fluctuations among the variables examined. The influence of these variables is mostly over the central and the south Indian regions. Hence, the variables examined are specially useful in predicting the rainfall indices of these regions.

The authors wish to acknowledge the valuable suggestions and guidance of Shri D.R. Sikka, F.A.Sc., Director, Indian Institute of Tropical Meteorology, Pune. They are also thankful to Dr. S.S. Singh, Head, Forecasting Research Division for providing necessary facilities and encouragement. Thanks are also due to Smt. C. Bardhan for typing the manuscript.

REFERENCES

Barnett, T. P. & Preisendorfer, R.W., (1978), *J. Atmos. Sci.*, **35**: 1771–1787.
Bedi, H.S. & Bindra, M. M. S., (1980), *Tellus*, **32**: 296–298.
Gray, W. M., (1983), Colorado State University, Atmos. Sci. Paper No. 370.
Jones, P. D., (1985a), *Climate Monitor*, **14**: 14–21.

Jones, P.D. (1985b), *Climate Monitor*, **14**: 43–50.
Jones, P.D. (1985c), *Climate Monitor*, **14**: 132–140.
Mooley, D.A. & Parthasarathy, B. (1983), *Mon. Wea. Rev.*, **111**: 967–978.
North, G. R., Bell, T. L., Cahalan, R. F. & Moeng, F. J., (1982), *Mon. Wea. Rev.*, **110**: 669–706.
Paolino, D. & Shukla, J., (1981), *WMO Tech. Report on Tropical Drought*, 41–48.
Rasmusson, E. M. & Carpenter, T. H., (1983), *Mon. Wea. Rev.*, **111**: 517–528.
Subbramayya, I., (1968), *J. Met. Soc. Japan*, **46**: 77–84.
Shukla, J. & Paolino, D., (1983), *Mon Wea. Rev.*, **111**: 1830–1837.
Sikka, D.R. & Prasad, K. D., (1981), *J. Climatol.*, **1**: 367–379.
Trenberth, K. E., (1976), *Quart. J. Roy. Meteor. Soc.*, **102**: 639–653.
Walker, G.T., (1924), *IX Mem. India. Met Dept.*, **24**: 333–345.